



Prototype Algorithm Development for Innovative Sensor Technology

SUMEIA ASSENAI



**KTH Information and
Communication Technology**

Prototype algorithm development for innovative sensor technology

SUMEIA ASSENAI

Master of Science Thesis

Embedded Systems
School of Information and Communication Technology
KTH Royal Institute of Technology

Stockholm, Sweden 2017

Examiner: Mark T. Smith

Abstract

Preterm infants are sensitive to incorrect levels of oxygen in the blood. Thus, the oxygen levels need to be monitored continuously. The most commonly used method today has several limitations and therefore constant blood tests has to be taken.

Neosense Technologies AB has developed an electrochemical sensor that measures blood oxygen tension continuously and in real time.

This thesis aims to develop a prototype algorithm to derive cardiac output based on dynamic changes in inhaled fraction of oxygen and the corresponding change in arterial oxygen tension using the electrochemical sensor.

Two measurements were done using the sensor to measure the step response of partial pressure of oxygen to obtain data to develop the algorithm. Using the obtained data, two algorithms were developed and from the validation analysis one of the algorithms were chosen due to significant better results.

Referat

För tidigt födda barn är känsliga för felaktiga syrgasnivåer i blodet. Därför krävs det noggranna och kontinuerliga mätningar. Dagens metoder är begränsade och ständiga blodprover behöver tas.

Neosense Technologies AB har utvecklat en sensor som mäter syrehalten i blodet kontinuerligt och i realtid.

Syftet med detta examensarbete är att utveckla en prototypalgoritm för att härleda hjärtminutvolymen baserat på dynamiska förändringar i syrehalten i inandningsluften och den motsvarande syrgasnivån i blodet med hjälp av den elektrokemiska sensorn.

Två mätningar gjordes med hjälp av sensorn där stegsvaret för partialtrycket av syre mättes för att erhålla data för algoritmutvecklingen. Med hjälp av den erhållna datan utvecklades två algoritmer och från valideringsanalysen valdes en av algoritmerna på grund av betydande bättre resultat.

Acknowledgment

I would like to thank my supervisors at Neosense Technologies AB for giving me the chance to conduct my thesis at the company and for their time, support and help with the project. I would also like to thank my examiner Mark T. Smith for the support and guidance.

Stockholm, 2017

Sumeia Assenai

Contents

1	Introduction	1
1.1	Background	1
1.2	Problem statement	2
1.3	Problem	2
1.4	Purpose	2
1.5	Goal	2
2	Methodology	3
3	Theoretical Framework	5
3.1	Blood oxygenation	5
3.2	Fraction of inspired oxygen	6
3.3	Arterial Oxygen Tension	6
3.4	Cardiac Output	6
3.4.1	Invasive methods	6
3.4.2	Minimally invasive methods	8
3.4.3	Non invasive methods	10
4	Prototype Algorithm Development	13
4.1	Overview	13
4.2	Gas mixing system	14
4.3	Software	15
4.4	Measurement setup	16
4.5	Calibration of sensor	16
4.6	Hypothesis of time consumption	17
4.6.1	Hypothesis #1	17
4.6.2	Hypothesis #2	19
4.7	Estimation of parameters	19
4.7.1	Measurements	19
4.7.2	Estimation of parameters of hypothesis #1	21
4.7.3	Estimation of parameters of hypothesis #2	23
4.8	Fluid flow calculation	26
4.9	Diffusion of gas	27
4.9.1	Diffusion of gas in a tube	27
4.9.2	Diffusion of gas in the lungs	29
5	Analysis	31
5.1	Validation Analysis	31

6 Conclusion and Future work	33
6.1 Conclusions	33
6.2 Development drawbacks	33
6.3 Future work	34
Bibliography	35

1

Chapter 1

Introduction

1.1 Background

Preterm infants are sensitive to too high or too low levels of oxygen in the blood. Hence measuring arterial oxygen tension correctly and continuously is important to be able to give suitable oxygen therapy. Too low oxygen levels increase the risk for brain damage such as cerebral palsy and too high levels increase the risk for eye damage (retinopathy of prematurity) [1].

The most commonly used non-invasive method for measuring oxygen saturation is pulse oximeter. This method has many advantages but also several limitations which leads to inaccurate measurements [2]. The limits which the amount of oxygen should be within, to minimize risks are narrow and therefore the accuracy is of utmost importance.

Neosense Technologies has developed an electrochemical sensor that measures blood oxygen tension, which apposed to oxygen saturation, is a direct indicator of oxygen exchange. Monitoring of oxygen tension in real-time is expected to improve oxygen therapy significantly for premature babies, since this variable is expected to effectively control oxygen supply within safe limits. The sensor is placed at the tip of an umbilical catheter, and can be used for up to 10 days [3].

Cardiac output is a parameter that gives fundamental information when investigating cardiovascular system. The most used method today to measure cardiac output is thermodilution, which is used together with a pulmonary artery catheter (PAC). This method is invasive and there are many complications related to pulmonary artery catheterization, including infections, arrhythmia, pulmonary artery rupture and vein thrombosis [4].

The idea is that the sensor, developed by Neosense Technologies, could also be used for measuring cardiac output. It is less invasive and the risks that are related to PAC are avoided.

1.2 Problem statement

The project will develop a transfer function to derive cardiac output based on dynamic changes in inhaled fraction of oxygen and the corresponding change in arterial oxygen tension.

1.3 Problem

To be able to measure cardiac output continuously and in real-time for a longer period of time (more than 5 days) without using pulmonary arterial catheter and without putting the patient at risk, using the sensor that Neosense Technologies has developed.

1.4 Purpose

The scope of this thesis is to develop a prototype algorithm for estimation of cardiac output, and test the algorithm in a test lab environment using saline (salt water).

1.5 Goal

The goal of this project is to develop a prototype algorithm for the estimation of cardiac output. The algorithm is derived based on theoretical calculations and hypothesis.

Simulations and measurements using the sensor to measure arterial oxygen tension with variation in inhaled fraction of oxygen is going to be done to validate the prototype algorithm.

2

Chapter 2

Methodology

The project was divided into three phases:

1. Literature study
2. Prototype algorithm development
 - Hardware implementation
 - Software
 - Prototype algorithm
 - Data collection
3. Model validation

The literature study was conducted by searching for scientific articles and books in the scope of this thesis to provide background facts that facilitates understanding the thesis project. Moreover, the literature study provided an overview of techniques for the measurement of cardiac output.

The second phase consisted of implementation of the gas mixing system, which enabled more precise control over the levels of inhaled fraction of oxygen. The gas mixing system consisted of a low-pass filter and two flow regulators controlled by an Arduino microcontroller. The system software was developed in MATLAB. The main functions of the software were enabling the operator to give input data and displaying the measured oxygen levels, inputs and outputs from the flow regulators and the calculated fluid flow. The next task in this phase was to develop a mathematical prototype algorithm with unknown parameters using the laws of physics. The last task was to perform measurements to collect data to validate the prototype algorithm.

In the third phase the collected data was analysed and the prototype algorithm models were validated.

3 Chapter 3

Theoretical Framework

This chapter provides background knowledge relevant for the thesis.

This chapter begins with essential information about blood composition, blood oxygenation and transportation of oxygen in the circulatory system. In the next section cardiac output is described and an overview of current cardiac output monitoring methods are given.

3.1 Blood oxygenation

The amount of blood of an adult is 4-4.5 L in women and 4.5-5 L in men. The blood is composed of blood cells, which are erythrocytes (red blood cells), leukocytes (white blood cells), thrombocytes (platelets), and blood plasma which is the fluid of the blood where proteins, hormones, nutrients, gases are dissolved in. The plasma consists also of plasma proteins, which facilitates transport of molecules that are insoluble in water by binding to them. The main functions of the blood is to transport various substances including oxygen, carbon dioxide, hormones, vitamins and regulation of the temperature of the body and immune defense [5].

The main function of the red blood cells is transportation of oxygen and carbon dioxide. The white blood cells, which are divided into six cell types, participates in the nonspecific and the specific immune system and the platelets are required for hemostasis [5].

In adults the development of red blood cells occurs in bone marrow and in fetuses the development occurs in the spleen and the liver [5].

There are two forms in which oxygen is transported in blood, bound to the hemoglobin in red blood cells and dissolved in plasma. About 98% of the transported oxygen is bound to hemoglobin.

Hemoglobin is a protein molecule that is made up of four globulin chains. Each globulin chain is bound to a heme group which consists of an iron ion inside a porphyrin compound. The inhaled oxygen, which diffuses into the capillaries surrounding the alveoli in the lungs, binds to the iron ion in the heme-group [6].

3.2 Fraction of inspired oxygen

Oxygen in air is often expressed as fraction of inspired oxygen (F_iO_2) which is the percentage of oxygen in inspired air. There is 20.9% oxygen in natural air and it is usually written in decimal form 0.21. In oxygen therapy the F_iO_2 is higher than 0.21.

3.3 Arterial Oxygen Tension

The natural air that is breathed is a combination of oxygen, nitrogen and carbon dioxide. The pressure of all gases at sea level is 765 mmHg. Partial pressure of oxygen in air at sea level is $765 * 0.21$ since oxygen in air is 21%.

Partial pressure of oxygen in a fluid is an equivalence to the partial pressure of oxygen in air. In arterial blood the partial pressure of oxygen is an equilibrium of pO_2 between the alveoli and the pulmonary capillary blood. This is usually between 75 mmHg and 100 mmHg.

3.4 Cardiac Output

Cardiac output is the volume of blood pumped by the heart per time unit, usually per minute. It is calculated as heart rate multiplied by stroke volume. Cardiac output is about 5.6 L per minute, in an adult individual [5]. Cardiac output is considered to be one of the most important parameter for hemodynamic monitoring since it is an indicator of how well the heart meets the demands of the body and how well the body is oxygenated [8].

There are many methods developed for measuring cardiac output; invasive, minimally invasive and non-invasive. The gold standard method is thermodilution [8]. The invasive methods are dilution techniques and the Fick method, the non-invasive methods are oesophageal doppler, partial carbon dioxide rebreathing, pulse contour analysis, thoracic bioimpedance and thoracic bioreactance.

3.4.1 Invasive methods

Fick Method

The first method to determine cardiac output was described by Adolph Fick in 1870 [7]. The method is based on the principle that the total uptake or release of a substance by an organ is the arteriovenous concentration difference and the blood flow through the organ. In this case, the substance is oxygen. The oxygen consumption by an organ is the product of cardiac output and arteriovenous oxygen difference [8]. The equation for calculating cardiac output:

$$CO = \frac{VO_2}{CaO_2 - CvO_2} \quad (3.1)$$

where VO_2 is oxygen consumption, CaO_2 is arterial oxygen content and CvO_2 is mixed venous oxygen content [11]. The arteriovenous oxygen difference is obtained from a sample of arterial blood and mixed venous blood from pulmonary artery [8].

This method is usually not suitable for critically ill patients due to instable haemodynamic status or because they require ventilatory conditions of high fractional inspired oxygen [7].

Thermodilution method

Dilution techniques requires a pulmonary artery catheter and an injection of some indicator. An indicator with a known volume and a known concentration is injected into the blood. The concentration of the indicator in the blood is measured over a time and from that the volume of the blood is then calculated according to the formula:

$$C_1 * V_1 = C_2 * V_2 \quad (3.2)$$

where C_1 is the known concentration of the indicator, V_1 is the known volume of the indicator, C_2 is the measured concentration of the indicator in the injected fluid and V_2 is what will be calculated, the volume of the fluid which has the indicator [9].

In thermodilution the indicator is temperature. A fluid with a known temperature is injected and mixed with the blood. There is a thermistor that registers the temperature at the tip of the catheter. The results are presented in a temperature-time curve. Cardiac output is then calculated by the Stewart-Hamilton formula: [9]

$$\text{Cardiac output} = V_1 \times (T_b - T_i) \times (\text{computation constant}) / [\text{integrated area of the measured temperature change over time } (T_2)]$$

where:

- V_1 = the volume of the injectate
- T_b = baseline blood temperature
- T_i = temperature of the injectate

Even though thermodilution using pulmonary artery catheter is considered a gold standard method, it is associated with many risks, including pneumothorax, pulmonary artery rupture, knotting and thrombosis, infections and valve injury [10].

Continuous cardiac output measurement can be accomplished by a modified thermodilution technique using a specially designed pulmonary artery catheter. The modification is copper filament in the catheter. The catheter remains in the right cardiac ventricle to obtain continuous measurements. The blood is periodically heated and a thermistor near the catheter tip measures the temperature [10].

The main advantages of continuous cardiac output measurement using a heated filament over a single thermodilution measurement are many. The measurements are done continuously and parameters as stroke volume, systemic vascular resistance and mixed venous saturation can also be calculated continuously [10].

A common disadvantage of using a pulmonary artery catheter is increased stress to the cardiac function since the catheter must be positioned through the cardiac valves and might cause valve leakage. Another disadvantage is increased risk for infection. Today the thermodilution technique is very seldom used at intensive care units.

3.4.2 Minimally invasive methods

Oesophageal Doppler

Oesophageal Doppler is a measurement technique that uses ultrasound and doppler effect to measure blood flow velocity in descending aorta. A transducer that is placed on a probe, is inserted orally and advanced until it reaches mid-thoracic level and then rotated until the transducer is facing the aorta [12].

The probe works as both the transmitter and receiver and uses a frequency of 4 MHz. This means that only one crystal is used for sending and receiving the ultrasound signals, which decreases the risk of error introduced by spacing of separate devices [14].

The second device that is used in this measuring technique is a waveform analyser. The analyser analyses the received signals and the frequencies and presents the results in a graphical and numerical form. A waveform is presented, with velocity on Y-axis and time on X-axis. Numerical information includes cardiac output, stroke volume, peak velocity and heart rate [14].

Calculating cardiac output depends on two important assumptions. The first assumption is the cross-sectional area of the descending aorta. The second assumption is the blood distribution before and after the measuring point on the aorta. With these two assumptions and parameters as the heart rate and stroke distance cardiac output and stroke volume can be derived [14].

A limiting factor to this method is that the resulting waveform is dependent on a correctly placed probe to obtain a correct signal [10]. The assumption of a fixed amount of the blood that goes to the head and the rest to the descending aorta differs in hemodynamically unstable patients [15].

Since there's no gold standard method among the noninvasive measuring methods, oesophageal doppler has been compared with PAC and the results agreed with PAC [14].

Partial carbon dioxide rebreathing

Partial carbon dioxide rebreathing method uses Fick's principle with carbon dioxide as the indicator gas. The venous carbon dioxide is calculated from the difference between inspired and expired gases after one minute of ventilation [8].

Fick equation for carbon dioxide:

$$CO = \frac{VCO_2}{CaCO_2 - CvCO_2} \quad (3.3)$$

where VCO_2 is the carbon dioxide consumption, $CvCO_2$ is the venous carbon dioxide concentration and $CaCO_2$ is the arterial carbon dioxide consumption. The arterial carbon dioxide concentration is estimated from end-tidal carbon dioxide [8].

Novamatrix Medical Systems developed a cardiac output monitor, named NICO, using Fick's principle. A circuit is connected to the ventilator with a carbon dioxide sensor, an airflow sensor and a rebreathing valve. Every three minutes the partial rebreathing is initiated by opening the valve [10].

The advantages of this method is enabling continuous monitoring of cardiac output with minimal invasiveness. However, the NICO system is limited to intubated patients without severe abnormality in gas exchange [11].

Pulse Contour Analysis

Pulse contour analysis is based on measuring pulse pressure in an artery to derive a waveform which is proportional to the stroke volume [10]. There are three systems based on this principle; Non-calibrated arterial contour analysis technique, PiCCO system and LiDCO system.

Non-calibrated arterial contour analysis technique: The system uses an invasive blood pressure sensor connected to an arterial line and a monitor. This method is minimally invasive and only uses an arterial line and the system does not need any calibration [11].

The calculating algorithm is based on the linearity between stroke volume and pulse pressure:

$$SV = SD_{AP} * \mu \quad (3.4)$$

Where SD_{AP} is the standard deviation of data points that reflects pulse pressure and μ is the conversion factor that depends on arterial compliance, mean arterial pressure and waveform characteristics [10].

The advantages of this system are that it enables continuous cardiac output monitoring and it is less invasive. Accuracy is however limited in patients with severe arrhythmia, unstable patients and in patients with conditions disturbing the arterial waveform [11].

PiCCO system: The PiCCO system uses a combination of pulse contour analysis and transpulmonary thermodilution technique. Both central venous and arterial cannulation are required for the measurement. Cold saline is injected via central venous cannula and the temperature change is registered by the thermistor tip catheter in femoral artery. The system requires manual calibration every 8 hours and more often in unstable patients [10][11].

An advantage PiCCO has over pulmonary artery catheter is that PiCCO is more useful in pediatrics due to pulmonary artery catheter is too big. The method is independent of respiratory and ventilator cycles and validation studies show a good agreement with PAC [10][11].

LiDCO system: The LiDCO system uses lithium as indicator in combination with pulse contour analysis for continuous monitoring of the stroke volume (SV). This technique requires a venous central line and arterial catheter, which has a lithium sensor attached to it. Lithium chloride is injected into the venous line and the arterial concentration is measured. Cardiac output is then calculated from a lithium concentration time plot [10][11].

The system requires calibration every 8 hours and when major hemodynamic changes occur [10].

The measuring method has been studied in relation with PAC and found being in good correlation [10]. However, the accuracy is compromised in some cases, including patients with arrhythmia and patients receiving lithium therapy [11].

3.4.3 Non invasive methods

Thoracic bioimpedance

This method measures cardiac output by measuring electrical resistance across the thorax by sending a low-amplitude high-frequency electrical current and calculating the stroke volume. Six electrodes are used, placed on the neck and lower thorax. The measured bioimpedance is indirectly proportional to the amount of fluid in the thorax [10].

The advantage of this method is that it is totally noninvasive monitoring method [11]. However, the measurements from bioimpedance have been found inaccurate in the intensive care unit and in other environments where there are significant electric noise and in patients with increased lung water. It has also been found to have poor agreement between thoracic bioimpedance and thermodilution. Any movements from the patient and improper placement of the electrodes also gives inaccurate measurements [15].

Thoracic bioreactance

Thoracic bioreactance is the further development of the thoracic bioimpedance method. This method overcomes the limitations that thoracic bioimpedance has such as external interference. The measurements are done using two dual-electrodes placed on the chest, one electrode sends alternating current with the frequency 75 kHz and the other electrode amplifies the voltage input to detect the signal. The system measures the time delay between the two signals. The obtained signals are correlated with aortic blood flow [10][11].

Limitations to this method are signal interference by electrocautery and loss of signals when the flow is low. However, bioreactance is easy to use in intubated patients, patients with arrhythmia, patients in the intensive care unit, operating room and emergency room. The method is completely noninvasive, measures cardiac output continuously and has good correlation with PAC [10][11].

4 Chapter 4

4 Prototype Algorithm Development

4.1 Overview

The developed algorithm derives cardiac output based on dynamic changes in inhaled fraction of oxygen and the corresponding change in arterial oxygen tension. In other words, how long does it take from a change in F_iO_2 has occurred until the the corresponding change in arterial oxygen tension is obtained.

The system has been divided into three blocks, see figure 4.1. The first block consists of the gas mixing system which acts as the ventilator. Input of this block is the required fraction of oxygen in the gas and the required total flow of the gas. The output of the first block is the partial pressure of the oxygen in the gas before it is inhaled.

The second block corresponds to the airways and lungs in the patient. In this block a diffusion of gas will occur and an algorithm is developed to calculate the partial pressure of oxygen in the alveoli depending on the volume of the airways and volume of the lungs.

The third block consists of the blood system and the sensor measuring the changes in the arterial oxygen tension. The algorithm used in this block derives cardiac output depending on the obtained changes in the arterial oxygen tension.

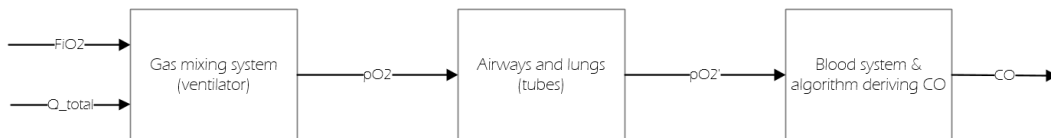


Figure 4.1: Block diagram describing the system

4.2 Gas mixing system

The gas mixing system is used to control the gas flow and the concentration levels of the oxygen. The gas mixing system is composed of two flow regulators, Aera FC-7700 [16], where one controls the air flow and the other controls the nitrogen flow. Both of the regulators are controlled by a microcontroller, Arduino Uno Rev 3, which is programmed using Matlab.

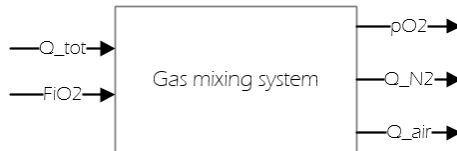


Figure 4.2: Block diagram with inputs/outputs of the gas mixing system

Input parameters for the gas mixing system are the total gas flow and the required fraction of oxygen. The program calculates the corresponding flows of air and nitrogen and regulates it. Figure 4.2 shows the inputs and the outputs of the gas mixing system and figure 4.3 shows a detailed block diagram of the gas mixing system.

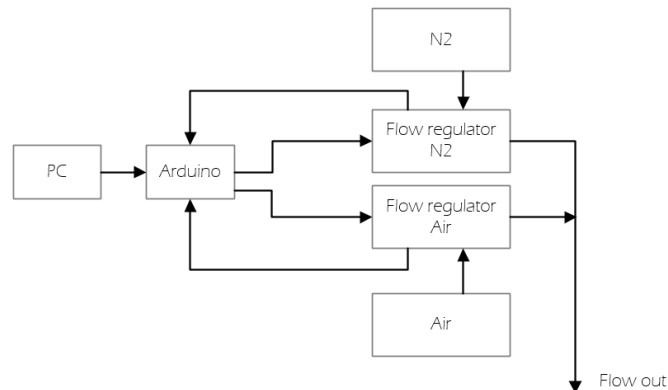


Figure 4.3: Block diagram describing the gas mixing system

The flow regulators receive only analog signals. The Arduino microcontroller has only digital and PWM outputs. To obtain an analog signal, PWM output was used together with a low pass filter, which can be seen in figure 4.4.

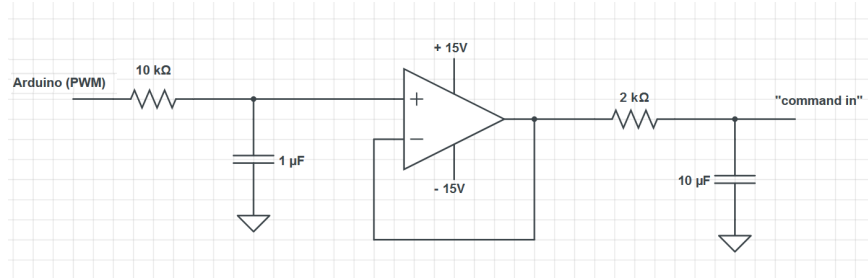


Figure 4.4: Low pass filter

4.3 Software

A graphical user interface was developed in Matlab to communicate with the Arduino microcontroller and to display different outputs.

The inputs of the program are information needed to control the flow regulators, such as the the total flow volume and required oxygen level.

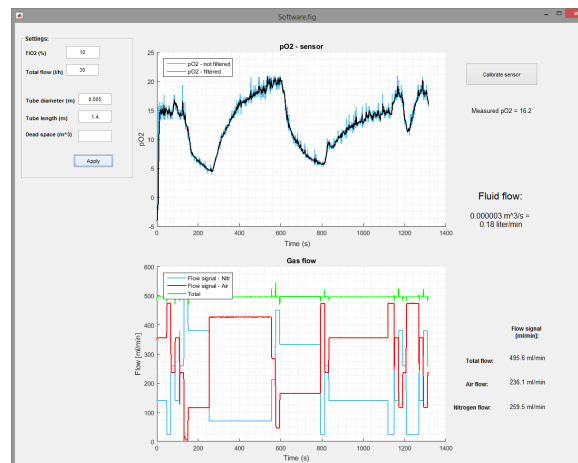


Figure 4.5: Screenshot of the software

As it can be seen in Figure 4.5 the program displays two graphs, the upper diagram shows the oxygen level measured by the sensor and the lower graph is a graphical display of the gas flows from the flow regulators. The second diagram is mainly to check that the flows obtained by the regulators are what the user entered in the beginning of the program and to see the changes since the start of the program. Both graphs plot real time data.

The program runs in an infinite loop and the user is able to change the input values any time and the program continues with the new inputs without starting over.

4.4 Measurement setup

The materials used in the measurement setup are: a pump, an oxygen sensor, an oxygenator and a gas mixing system. The gas mixing system is described in more details in section 4.2. Figure 4.6 shows how the system is connected.

The system consists of two subsystems, one subsystem for the gas and one subsystem for the fluid (saline). Both the gas and the saline go through the oxygenator, where the oxygenation of the saline occurs.

The pump which is used is a peristaltic pump (Manufacturer: ISMATEC. Model: MSC-WM5 [17]), and the oxygenator is from Medos, model: hilite 2400 LT [18].

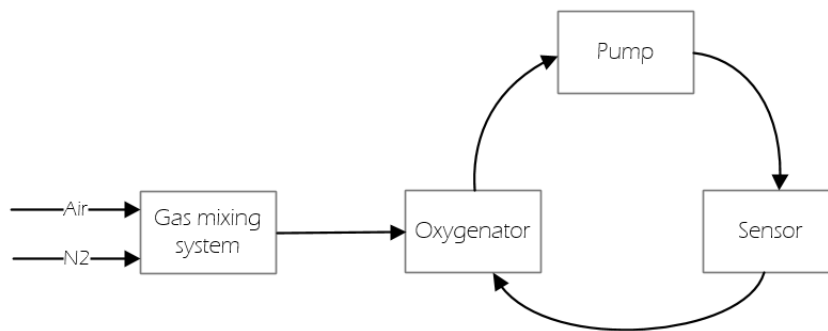


Figure 4.6: Measurements setup

The measurement setup represents a patient connected to a ventilator. The gas mixing system symbolizes the ventilator and the tubes from the gas mixing system to the oxygenator symbolizes the airways and the lung volumes. The fluid system with the pump and oxygenator symbolizes the circulatory system including the heart and the lungs. The oxygenation of the saline occurs in the oxygenator by a gas exchange between the gas and the fluid until an equilibrium is reached.

4.5 Calibration of sensor

Since the sensor needs to be calibrated before each measurement, a calibration function was implemented in the software. A look-up table with F_iO_2 and the corresponding A/D value was set up, and for the values that are not in the table, a linear spline function was used to derive the exact F_iO_2 based on values from the calibration table.

4.6 Hypothesis of time consumption

The next step is to find out how long time it takes for the gas to go from the gas mixing system, through the tubes, to the oxygenator and out to the sensor.

The system can be divided into two separate systems, with the oxygenator as a common part. The first system consists of the gas mixing system and the oxygenator, and the second system consists of the oxygenator, the pump and the sensor, which is the loop that can be seen in figure 4.7.

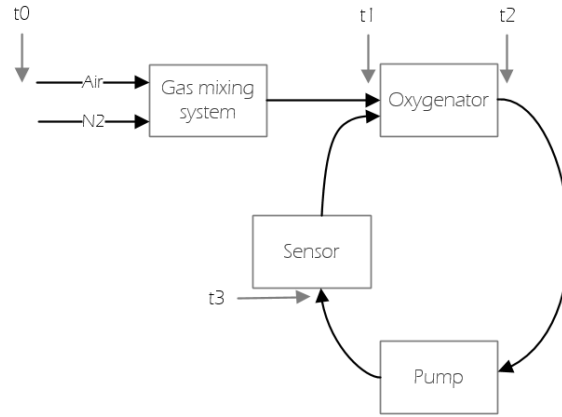


Figure 4.7: Diagram of the system with timestamps

Calculations of time consumption were based on two hypotheses.

4.6.1 Hypothesis #1

The time it takes for the gas with a volume flow rate of Q to travel through a tube with the length of L , the radius r and the volume of V :

$$V = L * A = L * \pi * r^2 \quad (4.1)$$

$$V = \int_0^t Q dt = L * \pi * r^2 \quad (4.2)$$

$$Q * t = L * \pi * r^2 \quad (4.3)$$

$$t = \frac{L * \pi * r^2}{Q} \quad (4.4)$$

$$t_{gas} = \frac{V_1}{Q_{gas}} \quad (4.5)$$

where:

- t_{gas} = time consumption
- V_1 = volume of the gas tube
- Q_{gas} = the volume flow rate of gas

This time consumption corresponds to t_1 in Figure 4.7.

In the second system, where the saline flows, the time it takes for the oxygen to reach the sensor depends on the volume flow rate of the saline, which depends on the velocity of the saline and the cross sectional area, A , of the tube in the motor. The velocity of the saline is determined by the radius of the rotor of the motor and angular velocity.

$$velocity_{saline} = r_{rotor} * \omega = r_{rotor} * 2\pi * f \quad (4.6)$$

$$velocity_{saline} = r_{rotor} * 2\pi * rpm \quad (4.7)$$

$$Q_{saline} = v_{saline} * A = r_{rotor} * 2\pi * rpm * \pi * r_{pump-tube}^2 \quad (4.8)$$

The information from (4.5) together with (4.8) for the volume flow rate of gas gives a formula that calculates the total time consumption:

$$t_{total} = \frac{V_1 + V_{oxy1}}{Q_{gas}} + \frac{V_2 + V_{oxy2}}{Q_{saline}} \quad (4.9)$$

where:

- V_1 = volume of the gas tube
- V_{oxy1} = the volume inside the oxygenator for the gas
- Q_{gas} = the volume flow rate of gas
- V_2 = the volume of the saline tube
- V_{oxy2} = the volume inside the oxygenator for the saline
- Q_{saline} = the volume flow rate of saline

All the above parameters, except for V_{oxy1} and V_{oxy2} , are known or can be calculated. To find the unknown parameters the method of least squares estimation was used.

4.6.2 Hypothesis #2

The second hypothesis for calculation of the time consumption was to set two coefficients (c_1 and c_2) which corresponds to the unknown volumes and any other factor that could affect the step response. With this method, the equations had the following forms:

$$t_{gas} = c_1 * \frac{V_1}{Q_{gas}} + \alpha_1 \quad (4.10)$$

$$t_{saline} = c_2 * \frac{1}{Q_{saline}} + \alpha_2 \quad (4.11)$$

where:

c_1 = unknown volume of oxygenator

V_1 = volume of the gas tube

α_1 = offset, the contributed time from the saline system

c_2 = unknown volume of oxygenator and saline tubes

α_2 = offset, the contributed time from the gas system

Combing (4.10) and (4.11) the following equation was obtained:

$$t_{total} = c_1 * \frac{V_1}{Q_{gas}} + \alpha_1 + c_2 * \frac{1}{Q_{saline}} + \alpha_2 \quad (4.12)$$

4.7 Estimation of parameters

Least square method was used to develop the mathematical functions further and find the unknown parameters that would have the best fit to data points obtained from measurements.

4.7.1 Measurements

Two sets of measurements were done to obtain measurement data. The first measurement corresponded to the first part of the equations, which was the step response to different volume flow rates of gas. The second measurement corresponded to the second part of the equation, which was the step response to different volume flow rates of saline.

Measurement #1

In the first measurement the step response of pO_2 in saline for different volume flow rate of gas is measured. The gas mixing system was used to regulate the volume flow rate of gas and the fraction of oxygen in the gas by changing the volume flow rate of the air and nitrogen. The total volume flow rate of the gas varied between 500 ml/min and 47 ml/min and the volume flow rate of saline was kept constant at $2.06 \cdot 10^{-3} \text{ m}^3/\text{s}$.

The results given in Table 4.1 show the step response in seconds for different volume flow rates of gas.

Volume flow rate of gas [ml/min]	Volume flow rate of gas [m^3/s]	Step response of pO_2 in saline [s]
500	$8.33 \cdot 10^{-6}$	34
450	$7.50 \cdot 10^{-6}$	35
400	$6.67 \cdot 10^{-6}$	37
350	$5.83 \cdot 10^{-6}$	39
300	$5.00 \cdot 10^{-6}$	41
250	$4.16 \cdot 10^{-6}$	44
200	$3.33 \cdot 10^{-6}$	52
150	$2.50 \cdot 10^{-6}$	63
100	$1.67 \cdot 10^{-6}$	75
47	$0.78 \cdot 10^{-6}$	116

Table 4.1: Step responses for various volume flow rate of gas with a constant volume flow rate of saline at $2.06 \cdot 10^{-5} \text{ m}^3/\text{s}$

Measurement #2

In the second measurement the step response of pO_2 for different volume flow rate of saline was measured while the volume flow rate of gas was kept constant at 500 ml/min. The volume flow rate of saline varied between $4.93 \cdot 10^{-5} \text{ m}^3/\text{s}$ and $1.23 \cdot 10^{-5} \text{ m}^3/\text{s}$.

The result given in Table 4.2 show the step response in seconds for different volume flow rates of saline.

RPM	Volume flow rate of saline [m ³ /s]	Step response [s]
120	4.93*10 ⁻⁵	25
110	4.52*10 ⁻⁵	26
100	4.11*10 ⁻⁵	27
90	3.70*10 ⁻⁵	28
80	3.29*10 ⁻⁵	29
70	2.88*10 ⁻⁵	30
60	2.47*10 ⁻⁵	34
50	2.06*10 ⁻⁵	35
40	1.64*10 ⁻⁵	37
30	1.23*10 ⁻⁵	41

Table 4.2: Step responses for various volume flow rate of saline and constant volume flow rate of gas at 500 ml/min

4.7.2 Estimation of parameters of hypothesis #1

Using observed data in Table 4.1 and ordinary least squares estimation method the parameters in the model are estimated. Since the model was built of two terms where each term calculates the time consumption in each system, the parameters are estimated in two steps. First step was to estimate the parameters in the gas system. This corresponded to:

$$t_{gas} = \frac{V_1 + V_{oxy1}}{Q_{gas}} + k_1 \quad (4.13)$$

The parameter k_1 in (4.13) corresponds to the time contributed from the saline system.

The following solution was obtain:

$$V_1 + V_{oxy1} = 71.7 \text{ ml}$$

$$k_1 = 27.9 \text{ seconds}$$

This means that the combined volume of the gas tubes and the volume inside the oxygenator for the gas is 71.7 ml. The volume of the gas tubes (from the gas mixing system to the oxygenator) is 45 ml, which means that the volume in the oxygenator is 26.7 ml.

The other parameter k_1 was the time it took for the oxygenation inside the oxygenator and the time it took for the oxygenated saline to reach the sensor. In this case, this time lapse was constant due to all parameters except for the volume flow rate of gas which was held constant during the measurement.

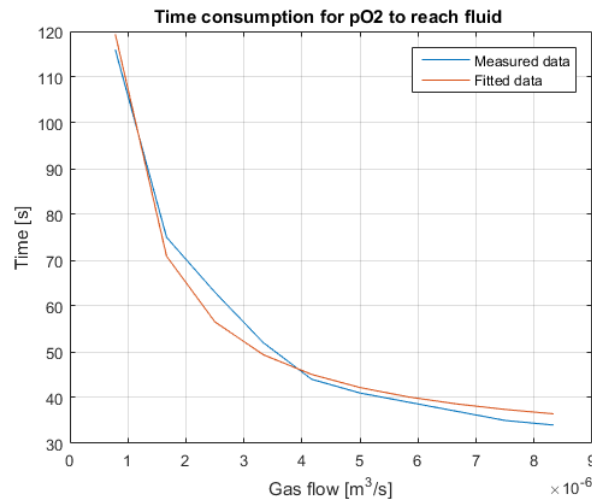


Figure 4.8: Graph displaying the observed data and the estimated model for various volume flow rate of gas

Figure 4.8 shows a line graph displaying the measured data. The graph also shows the line of best fit to the measured data using the parameters that were obtained using the least squares estimation method.

The next parameters to estimate were the parameters in the second part of the model which corresponds to the saline system:

$$t_{saline} = \frac{V_2 + V_{oxy2}}{Q_{saline}} + k_2 \quad (4.14)$$

The parameter k_2 in (4.14) corresponds to the time contributed from the gas mixing system.

Using observed data from Table 4.2 and ordinary least squares estimation method the following solution was obtained:

$$V_2 + V_{oxy2} = 265 \text{ ml}$$

$$k_2 = 20.9 \text{ seconds}$$

These values mean that the volume of saline contained inside the oxygenator is 190 ml due to the volume of the tubes of the saline is 75 ml.

The second parameter k_2 is the time it takes for the oxygenation and for the gas to reach the oxygenator from the gas mixing system.

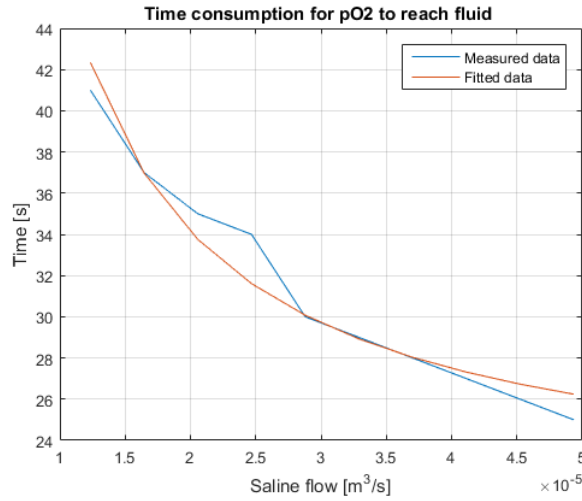


Figure 4.9: Graph displaying the observed data and the estimated model for various volume flow rate of saline

Figure 4.9 shows a line graph displaying the measured data. The graph also shows the line of best fit to the measured data using the parameters that were obtained using the least squares estimation method.

With the parameters estimated, the following model became:

$$t_{total} = \frac{V_1 + 2.67 * 10^{-5}}{Q_{gas}} + \frac{V_2 + 26.5 * 10^{-5}}{Q_{saline}} \quad (4.15)$$

4.7.3 Estimation of parameters of hypothesis #2

The same estimation process done in the previous section was done again in this section to the model from the second hypothesis, see (4.12).

Using observed data in Table 4.1 and Table 4.2 and ordinary least squares estimation method the parameters were estimated.

The obtained parameters are:

$$\begin{aligned} c_1 &= 1.59 \\ \alpha_1 &= 27.9 \\ c_2 &= 26.5 * 10^{-5} \\ \alpha_2 &= 20.9 \end{aligned}$$

Inserting obtained values in (4.12):

$$t_{total} = 1.59 * \frac{V_1}{Q_{gas}} + 27.9 + 26.5 * 10^{-5} * \frac{1}{Q_{saline}} + 20.9 \quad (4.16)$$

Figure 4.10 shows a graph displaying the measured data from the first measurement and the line of best fit to the measured data using the parameters that were obtained using the least squares method. The graph also shows the time constant α_1 .

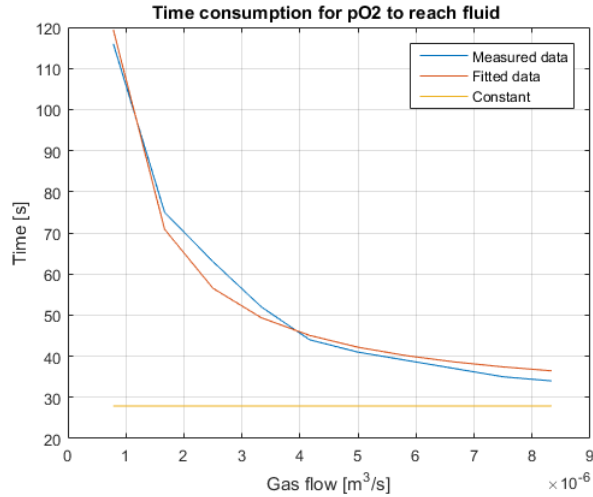


Figure 4.10: Graph displaying the observed data, the estimated model for various volume flow rate of gas and the time constant α_1

Figure 4.11 shows a graph displaying the measured data from the second measurement and the line of best fit to the measured data using the parameters that were obtained using the least square method. The graph also shows the time constant α_2 .

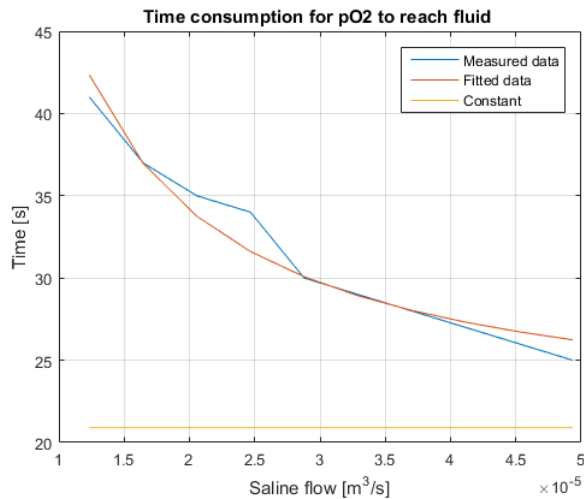


Figure 4.11: Graph displaying the observed data, the estimated model for various volume flow rate of saline and the time constant α_1

4.7 Estimation of parameters

After analysing the simulations and the calculations it appeared that the parameters α_1 and α_2 included the same factor twice.

In Figure 4.10, the volume flow rate of gas was the only varying parameter. This means that the time constant α_1 included the time for the oxygenation and the time consumption affected by the volume flow rate of saline.

In the second measurement the volume flow rate of saline was the varying parameter and the time constant α_2 included the time for oxygenation and the time contribution from the volume flow rate of gas.

With this reasoning, it was clear that it would be wrong to have both α_1 and α_2 in the equation. Instead of α_1 and α_2 , a new parameter was introduced, t_d and the model was rewritten into:

$$t_{total} = 1.59 * \frac{V_1}{Q_{gas}} + 26.5 * 10^{-5} * \frac{1}{Q_{saline}} + t_d \quad (4.17)$$

Observed data from Table 4.2 together with the obtained parameters were used to make an estimation of the new parameter. The model was rewritten into:

$$Q_{saline} = \frac{26.5 * 10^{-5}}{(t_{total} - t_d - (1.59 * \frac{V_1}{Q_{gas}}))} \quad (4.18)$$

The results given in Table 4.3 show the estimated parameter t_d for different volume flow rates of saline and Figure 4.12 shows the obtained data in a line graph.

RPM	Volume flow rate of saline [m ³ /s]	Step response [s]	t_d [s]
120	4.93*10 ⁻⁵	25	11.03
110	4.52*10 ⁻⁵	26	11.55
100	4.11*10 ⁻⁵	27	11.96
90	3.70*10 ⁻⁵	28	12.25
80	3.29*10 ⁻⁵	29	12.35
70	2.88*10 ⁻⁵	30	12.20
60	2.47*10 ⁻⁵	34	14.66
50	2.06*10 ⁻⁵	35	13.52
40	1.64*10 ⁻⁵	37	12.25
30	1.23*10 ⁻⁵	41	10.93

Table 4.3: Estimation of t_d for various volume flow rate of saline at a constant volume flow rate of gas at 500 ml/min

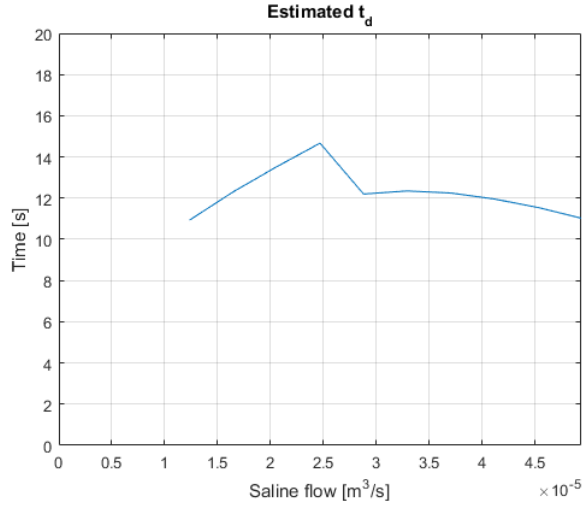


Figure 4.12: Graph displaying the estimated values for t_d at various volume flow rate of saline at a constant volume flow rate of gas at $8.33 \times 10^{-6} \text{ m}^3/\text{s}$

From the results above, the new parameter t_d was constant to a degree and could be roughly approximated to an average value. This led to the following model:

$$t_{total} = 1.59 * \frac{V_1}{Q_{gas}} + 26.5 * 10^{-5} \frac{1}{Q_{saline}} + 12.27 \quad (4.19)$$

4.8 Fluid flow calculation

The last step was to do the actual fluid flow calculations which, as mentioned in Section 4.4, corresponds to the cardiac output calculation in a patient in this system.

Using (4.15) and (4.19), the two models for calculation of volume flow rate of the fluid in the system were obtained:

$$Q_{fluid} = \frac{V_2 + 26.5 * 10^{-5}}{t_{total} - \frac{V_1 + 2.67 * 10^{-5}}{Q_{gas}}} \quad (4.20)$$

$$Q_{fluid} = \frac{26.5 * 10^{-5}}{t_{total} - 12.27 - 1.59 * \frac{V_1}{Q_{gas}}} \quad (4.21)$$

where:

- V_1 = volume of the gas tubes
- V_2 = the volume of the saline tube
- t_{total} = the total time consumption from a change in inhaled fraction of oxygen occurs until it reaches the sensor
- Q_{gas} = the volume flow rate of gas

4.9 Diffusion of gas

Diffusion of gas is a factor that could affect the concentration level of the oxygen in the gas and the time it takes for the diffusion to occur and therefore it was looked into to examine the impact it could have in the developed prototype algorithm.

4.9.1 Diffusion of gas in a tube

Change in the fraction of oxygen in the delivered gas, via the gas mixing system, leads to a diffusion occurs between the newly delivered gas and the available gas. Diffusion is a process where molecules are transported from one part of a system to another, usually from a higher concentration to a lower. In this case, diffusion occurs inside the tubes and it is primarily in the direction of the gas flow inside of the tubing, and therefore the diffusion is one-dimensional. This is described by Fick's second diffusion law:

$$\frac{\delta C}{\delta t} = D \frac{\delta^2 C}{\delta x^2} \quad (4.22)$$

where:

- C = the concentration [mol/m³], C is a function of time and position $C = C(x, t)$
- D = the diffusion coefficient [m²/s]
- t = time [s]
- x = position in the tube [m]

The solution to Fick's second law is selected on the basis of the boundary conditions and the number of dimensions. In this case, the boundary conditions are:

$$\begin{array}{lll} C(x, t) = C_0 & \text{at } t = 0 & 0 \leq x \leq \infty \\ C(x, t) = C_s & \text{at } t > 0 & x = 0 \\ C(x, t) = C_0 & & x = \infty \end{array}$$

The solution used:

$$\frac{C(x, t) - C_0}{C_s - C_0} = 1 - \operatorname{erf}\left(\frac{x}{\sqrt{4Dt}}\right) \quad (4.23)$$

$$C(x, t) = \left(1 - \operatorname{erf}\left(\frac{x}{\sqrt{4Dt}}\right)\right)(C_s - C_0) + C_0 \quad (4.24)$$

where:

- $C(x, t)$ = concentration at position x at time t
- C_0 = initial concentration
- C_s = concentration at $t > 0$ and $x = 0$
- D = diffusion coefficient [m^2/s]
- x = position [m]
- t = time [s]

In figure 4.13 the process of diffusion of gas was simulated. The time variable was constant at $t=20$ s and the position variable varied.

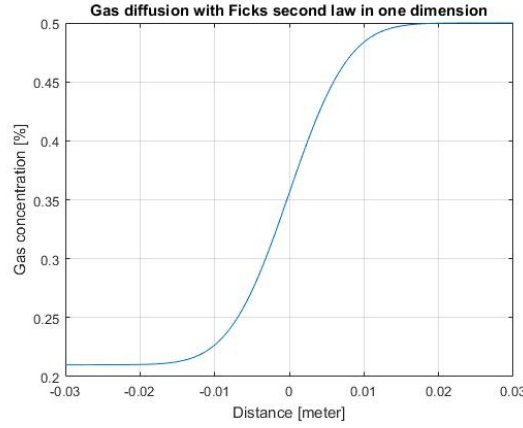


Figure 4.13: Gas diffusion with respect to position at time $t = 20$ s

Error function (erf) in (4.24) is a standard mathematical function, written as:

$$\operatorname{erf}(z) = \frac{2}{\sqrt{\pi}} \int_0^z \exp(-\eta^2) d\eta \quad (4.25)$$

Diffusion coefficient D depends strongly on temperature and since it is assumed that the temperature is constant, the diffusion coefficient is assumed to be constant.

The result of the analysis of the diffusion simulation, with the simplifications, is that the diffusion does not make a big impact on concentration changes in the gas. According to the simulation results the part inside the tube where the diffusion occurs spreads out only about 2 cm after 20 seconds. Depending on the used flow rate of

the gas, the gas is not always inside the tube long enough for the gas to diffuse for a longer time. Due to this conclusion, the impact of the diffusion is neglectable and not taken into account in the prototype algorithm development.

4.9.2 Diffusion of gas in the lungs

Diffusion of gases occurs in the lungs and on the way to the alveoli. The amount of time the gas is exposed to diffusion depends on the size of the lungs and the flow rate of the gas. The lung volume of interest to be taken into account is the total lung capacity, which varies depending on gender, age, length and weight.

This is not further discussed or taken into account in the calculations since it is out of the scope for the thesis.

5 Chapter 5

Analysis

5.1 Validation Analysis

Validation of the model was done using two validation methods: mean squares error and R^2 .

The mean squares error formula and the R^2 formula used to evaluate the models:

$$MSE = \frac{1}{N} \sum_{i=1}^N (\hat{y} - y_i)^2 \quad (5.1)$$

$$R^2 = 1 - \frac{\sum_{i=1}^N (\hat{y} - y_i)^2}{\sum_{i=1}^N (\bar{y} - y_i)^2} \quad (5.2)$$

where:

N = the number of data points

\hat{y} = the estimated values by the model

y_i = the observed values

\bar{y} = the mean value of observed values y_i

The results from the validation calculations are in the table below, see Table 5.1.

Validation method	MSE	R^2
Model 1	110.8	0.30
Model 2	24.8	0.37

Table 5.1: The validation analysis results

Comparing the two prototype models from the results in Table 5.1 it is clear that model 2 has a better fit based on the mean squares error method. However, the R^2

does not show a significant difference between the two models, even though model 2 has a higher R^2 , which indicates a higher percentage of the variance in the response variable is explained by the regression model. This means that model 2 is a better model in terms of better fit and validation analysis.

6

Conclusion and Future work

6.1 Conclusions

The developed prototype algorithm fulfills the aim of this project. It calculates an estimation of fluid flow and for this experiment setup the fluid calculations were accurate.

Two similar models, with different assumptions, were developed and evaluated. From the validation results one of the models gave significant better results than the other.

6.2 Development drawbacks

One main drawback in this project was the equipment used in the measurements. The pump used in this project was a peristaltic pump, which gave a pulsed flow of the saline. This made the sensor signal very noisy which made the estimation of the step response in the measurements harder and some values are more or less an assumption. A more smooth and consistent flow of the saline would probably give a less noisy sensor signal and in turn this would make the signal reading easier and more accurate.

Another drawback to the measurements was the sensor. There were two sensors available for the measurements but both sensors had been used for a long time. The sensors would sometimes stop work in the middle of the measurement sessions and they would have to be disconnected and connect the other sensor.

All the equipment needed for the measurements were not available from the start, which resulted in some waiting time, and when some of the equipment arrived they did not work properly. This problem was solved fast thanks to KTH lab.

6.3 Future work

Due to the limitations of the thesis project there were not many parameters that were taken into account in the prototype algorithm. There are many factors that should be taken into account or their impact on the calculations should be examined to obtain a more accurate prototype.

Further development of the prototype algorithm is summarized in the following points:

- As mentioned in section 6.2, the measurement data would be better and more reliable with more stable measurement setup and equipment.
- To further develop the algorithm it would be interesting to test the algorithm with changed parameter values such as the volume of the gas tube and the saline tube.
- It would be a good idea to develop the GUI further to automatically detect the time consumption for the sensor to detect the changes in the oxygen levels.

Bibliography

- [1] Meayoung Chang, 'Optimal oxygen saturation in premature infants', *Korean Journal of Pediatrics*, vol. 54(9), pp.359-362, Sep. 2011. [Online]. Available: <http://www.ncbi.nlm.nih.gov/pmc/articles/PMC3250600/> (DOI: 10.3345/kjp.2011.54.9.359). [Accessed Oct. 15, 2016].
- [2] Jubran A. 'Pulse oximetry', *Critical Care*, vol. 3(2), R11-R17, May 1999. [Online]. Available: <https://www.ncbi.nlm.nih.gov/pmc/articles/PMC137227/>. (DOI: 10.1186/cc341). [Accessed Oct. 15, 2016].
- [3] D. Callahan and P. Larsson, 'Improved care for premature babies', May 19, 2015. [Online]. Available: <https://www.kth.se/en/aktuellt/nyheter/fler-for-tidigt-foddabarn-kan-raddas-1.566126>. [Accessed Oct. 15, 2016].
- [4] D. Payen and E. Gayat, 'Which general intensive care unit patients can be benefit from placement of pulmonary artery catheter?', *Critical Care*, Nov. 27 2006. [Online]. Available: <https://www.ncbi.nlm.nih.gov/pmc/articles/PMC3226130/>. (DOI:10.1186/cc4925). [Accessed Oct. 15, 2016].
- [5] S. Silbernagl and A. Despopoulos, *Color of Atlas of Physiology*, 6th ed., Stuttgart New York: Thieme, 2009. ISBN 978-3-13-545006-3. [Online]. Available: <http://course.sdu.edu.cn/G2S/eWebEditor/uploadfile/20130328161819736.pdf>. [Accessed Oct. 15, 2016].
- [6] R.N. Pittman *Regulation of Tissue Oxygenation*. San Rafael (CA): Morgan & Claypool Life Sciences; 2011. Chapter 4, Oxygen Transport. [Online]. Available: <https://www.ncbi.nlm.nih.gov/books/NBK54103/>. [Accessed Oct. 15, 2016].
- [7] L. Mathews and K.R. Singh, 'Cardiac output monitoring'. *Annals of Cardiac Anaesthesia*, vol. 11, pp. 56-68, 2008. [Online]. Available: <http://www.annals.in/text.asp?2008/11/1/56/38455>. [Accessed Sept. 20, 2017].
- [8] M. Lavdaniti, 'Invasive and non-invasive methods for cardiac output measurement', *International Journal of Caring Sciences*, vol. 1(3), pp.112-117, Sep-Dec 2008. [Online]. Available: http://internationaljournalofcaringsciences.org/docs/Vol1_Issue3_02_Lavdaniti.pdf. [Accessed Oct. 15, 2016].
- [9] S. C. Haskins, *Cardiac Output Monitoring, in Advanced Monitoring and Procedures for Small Animal Emergency and Critical Care*, (eds J. M. Burkitt Creedon and H. Davis), Chichester, UK: John Wiley & Sons, Ltd, 2012. ISBN: 9781118997246 [Online] Available: <http://dx.doi.org/10.1002/9781118997246.ch12> (DOI: 10.1002/9781118997246.ch12). [Accessed Oct. 15, 2016].

- [10] Y. Mehta and D. Arora, 'Newer methods of cardiac output monitoring'. *World Journal of Cardiology*, vol. 6(9), pp. 1022-1029, Sep 2014. [Online]. Available: <https://www.ncbi.nlm.nih.gov/pmc/articles/PMC4176793/> (DOI:10.4330/wjc.v6.i9.1022). [Accessed Oct. 15, 2016].
- [11] L. Sangkum, G.L. Liu, L. Yu, et al., 'Minimally intensive or nonintensive cardiac output measurement: an update', *Journal of Anesthesia*, vol. 30(3), pp. 461-480, Jun. 2016. [Online]. Available: <https://doi-org.focus.lib.kth.se/10.1007/s00540-016-2154-9>. [Accessed Oct. 15, 2016].
- [12] B. P. Cholley and M. Singer, 'Esophageal Doppler: Noninvasive Cardiac Output Monitor', *Echocardiography*, vol. 20, pp. 763-769. Nov. 2003. [Online]. Available: <https://www.ncbi.nlm.nih.gov/pubmed/14641384>(DOI:10.1111/j.0742-2822.2003.03033.x). [Accessed Oct. 15, 2016].
- [13] Lester Augustus Hall Critchley (2013). Minimally Invasive Cardiac Output Monitoring in the Year 2012, Artery Bypass, Dr Wilbert S. Aronow (Ed.), InTech, DOI: 10.5772/54413. Available from: <https://www.intechopen.com/books/artery-bypass/minimally-invasive-cardiac-output-monitoring-in-the-year-2012>
- [14] D. A. Colquhoun, 'Oesophageal Doppler cardiac output monitoring: A longstanding tool with evolving indications and applications', *Best Practice & Research Clinical Anaesthesiology* Vol. 28(4), pp. 353-362, Dec 2014. [Online]. Available: <http://dx.doi.org.focus.lib.kth.se/10.1016/j.bpa.2014.09.007>. [Accessed Oct. 15, 2016].
- [15] P.E. Marik, 'Noninvasive cardiac output monitors: a state-of the-art review' *Journal of Cardiothoracic and Vascular Anesthesia*, vol. 27(1), pp. 121-134. Feb 2013. [Online]. Available: <https://www.ncbi.nlm.nih.gov/pubmed/22609340> (DOI: 10.1053/j.jvca.2012.03.022). [Accessed Oct. 15, 2016].
- [16] Hitachi Metals America, Ltd. [Online] Available: <http://www.hitachimetals.com/>. [Accessed Nov. 22, 2017]
- [17] Cole-Parmer GmbH. [Online] Available: http://www.ismatec.com/int_e/index.htm [Accessed Nov. 22, 2017]
- [18] XENIOS AG. [Online] Available: <https://www.xenios-ag.com/medos/> [Accessed Nov. 22, 2017]

